LA-UR-15-28681
Approved for public release; distribution is unlimited.

Title: SHINE Tritium Nozzle Design Activity 6, Task 1 Report

Author(s): Okhuysen, Brett S.
Pulliam, Elias Noel

Intended for: Report

Issued: 2015-11-05

SHINE Tritium Nozzle Design
Activity 6, Task 1 Report

Brett Okhuysen
Elias Pulliam

30 September 2015

Statement of Work

In FY14, we studied the qualitative and quantitative behavior of a SHINE/PNL tritium nozzle under varying operating conditions. The result is an understanding of the nozzle's performance in terms of important flow features that manifest themselves under different parametric profiles. In FY15, we will consider nozzle design with a focus on nozzle geometry and integration. From FY14 work, we will understand how the SHINE/PNL nozzle behaves under different operating scenarios. The first task for FY15 is to evaluate the FY14 model as a predictor of the actual flow. Considering different geometries is more time-intensive that parameter studies, therefore we recommend considering any relevant flow features that were not included in the FY14 model. In the absence of experimental data, it is particularly important to consider any sources of heat in the domain or boundary conditions that may affect the flow and incorporate these into the simulation if they are significant. Additionally, any geometric features of the beamline segment should be added to the model such as the orifice plate. The FY14 model works with hydrogen. An improvement that can be made for FY15 is to develop CFD properties for tritium and incorporate those properties into the new models.

The FY14 model focused on how changes in operating parameters such as nozzle pressure and target pressure affected flow phenomenology and consequently the amount of backflow in the line. For FY15, we propose to study some effects of geometry changes using the SHINE/PNL nozzle, which was the basis for the FY14 model, as a baseline. The purpose of considering geometry changes is to evaluate what nozzle features, either by design or consequence, contribute positively or negatively to the system performance.

Introduction

Phoenix Nuclear Laboratory (PNL) has designed a neutron generator in which an accelerator produces a beam that is directed at a gas target. To produce the beam, a vacuum is required. It is advantageous to pressurize the target gas to obtain a higher density. The higher density gas leads to a higher probability of collisions between the beam and target atoms, resulting in more efficient neutron generation. However, the low pressure of a vacuum and higher pressure of a target leads to flow of target gas from the chamber into the vacuum. This backflow wastes target gas and also results in premature beam collisions that occur outside the target chamber. To address this issue, PNL seeks to maximize the pressure drop between the target chamber at some pressure, e.g. 10 Torr, and the ISO100 bellows at some pressure several orders of magnitude lower, e.g. 50 mTorr, while simultaneously minimizing the backflow of target gas from the target chamber through the bellows.

A simplified version of this region of the beamline is shown in Figure 1. One method suggested in the literature[1,2,3] for obtaining this minimization is to add a nozzle to the beamline and create a flow counter to the right-to-left flow induced by the pressure difference between the target and the vacuum.

[1] Gasdynamic Measurements for the LASL Intense Neutron Source. Johnston, SC SAND77-8294 (1977).
[2] An Intense Neutron Source Facility using a Supersonic Jet Target. Cline, MC and Emigh CR, Presented at the First Topical Meeting on the Technology of Controlled Nuclear Fusion, San Diego CA (1974).
[3] Jet Target Intense Neutron Source. Meier, KL, LA-UR-77-3298 (1977).

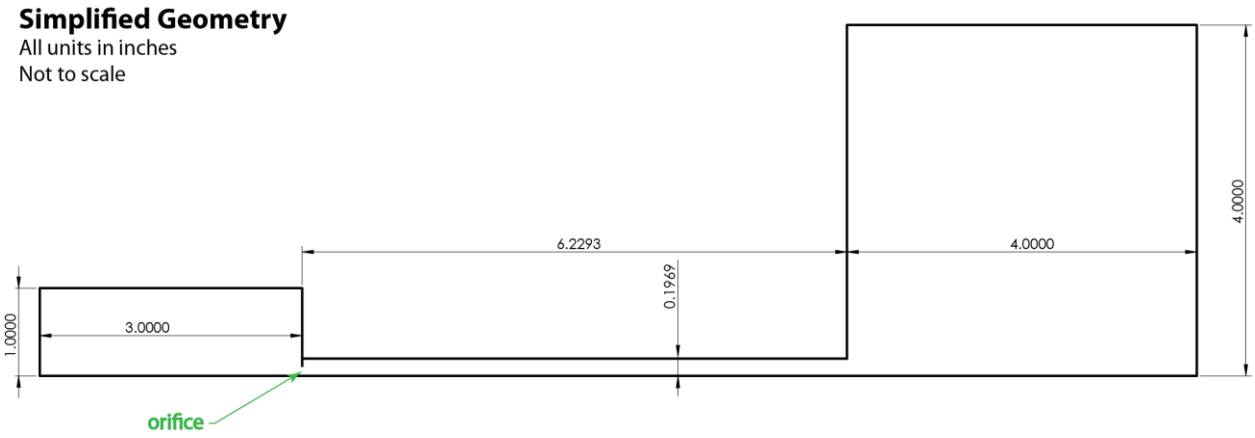

Figure 1: Simplified geometry of the beamline from the ISO100 bellows on the left to the target chamber on the right, connected by the KF40 bellows in the middle (with units in inches, not to scale).

The SHINE Nozzle

SHINE proposed a design to minimize backflow into the vacuum chamber by introducing a nozzle attached to the flow passage connecting the left hand side (LHS) vacuum chamber and right hand side (RHS) target chamber. The initial SHINE nozzle design is shown in Figure 2 and denoted nozzle-0. Modeling nozzle-0 proceeded in several steps. The nozzle was initially treated as a rectangular structure, with the cross-section shown in n Figure 2 extruded one meter and symmetric about the bottom axis. The CFD model was generated in two-dimensional Cartesian coordinates.

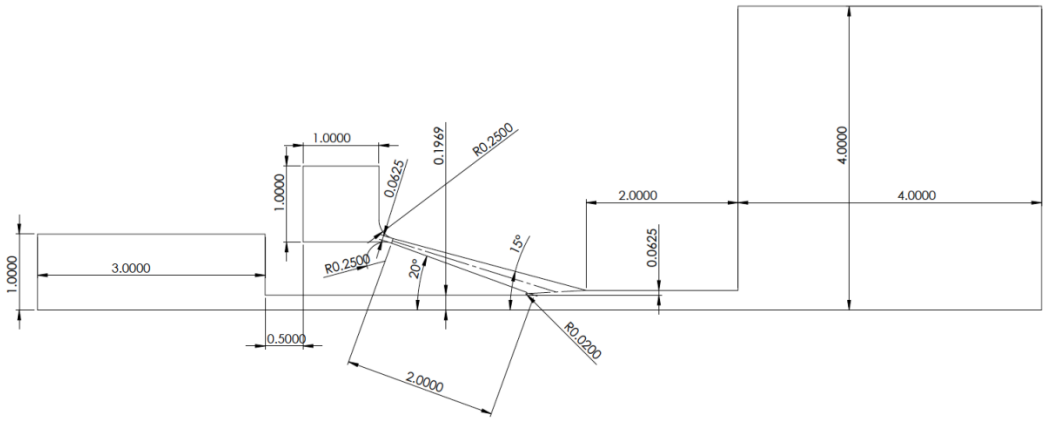

Figure 2: The initial Shine nozzle-0 design (with units in inches), not to scale.

In previous work, parameter studies were conducted on the nozzle-0 2D Cartesian model by varying nozzle reservoir inlet pressure for two target chamber (RHS) boundary pressures. The RHS pressure outlet condition was set to 10 Torr and nozzle inlet pressure was varied from 10 Torr to 750 Torr. The RHS pressure outlet condition was then set to 30 Torr and values of nozzle inlet pressure in the same range were selected. The first parameter study performed was for a ten Torr target. The pressure outlet boundary condition at the LHS of the domain was set to 50 mTorr. The pressure outlet boundary

condition at the RHS of the domain was set to 10 Torr. The pressure value at the pressure inlet boundary condition at the nozzle reservoir was varied and the resulting mass flow rate of hydrogen gas into the vacuum chamber was recorded. The results of this parameter study are shown in Figure 3.

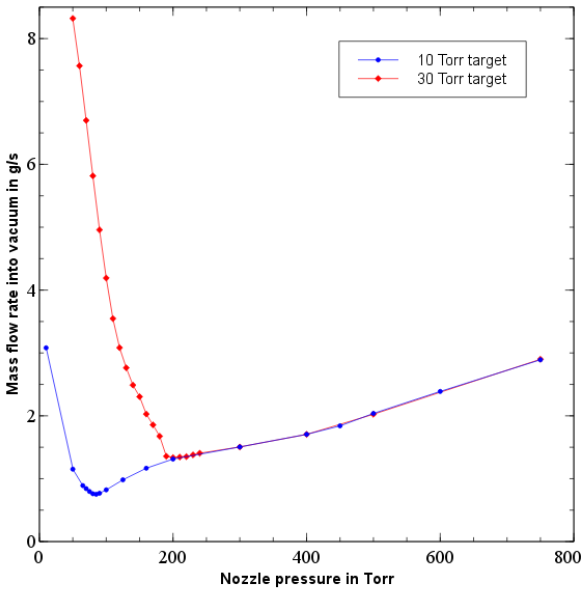

Figure 3: Comparison of the curves for mass flow rate verses nozzle pressure for the target pressures of 10 Torr and 30 Torr for the 2D Cartesian nozzle-0 model.

For both target cases considered, the performance curves were generated considering nozzle reservoir input pressures between 10 Torr and 750 Torr. A minimum flow rate was determined for intermediate nozzle input pressures for both target pressures. For the 10-Torr case, the minimum mass flux rate of 0.75 g/(s m) was calculated for an 85-Torr input pressure. For the 30-Torr case, a minimum mass flux rate of 1.33 g/(s m) was computed for an input pressure of 200 Torr.

Motivated by these results, the nozzle-0 geometry was implemented as an axisymmetric model with the same dimensions shown in Figure 2. The first step in the CFD analysis was to construct a geometric model of the system. This model was then used to generate a computational mesh of the geometry. A two-dimensional axisymmetric mesh was built using the ANSYS Gambit mesh generator tool. The resulting mesh of the model geometry is shown in Figure 4. The computational domain defined in the geometry model matches the design drawing except for a sharp corner, as noted in previous reports. Four boundary conditions were specified in Gambit. The horizontal top surface of the nozzle reservoir was set to be a pressure inlet condition. The left and right vertical surfaces at the extremes of the full domain were set to pressure outlet conditions. The line extending along the entire bottom of the domain denotes an axis of axial symmetry, and was set to be an axis condition.

For all subsequent analyses, LANL considered the compressible flow of hydrogen through the assembly. Hydrogen was modeled as an ideal gas. The analysis used a density-based solver with double precision. The analysis was performed using an implicit formulation of Roe-FDS type. The spatial discretization

was a least squares cell based gradient using second-order upwind for mass, momentum, energy, total kinetic energy (TKE), and dissipation rate. LANL used the K-omega SST turbulence closure with compressible effects enabled. The K-omega SST model uses K-omega to model turbulence near to walls, but blends between K-omega and K-epsilon models as positions away from the wall are considered. Away from walls, the selected closure limits to the standard K-epsilon model. To improve the speed and robustness of convergence to solutions, Fluent's solution steering was enabled. The supersonic parameter profile was used with full multi-grid (FMG) initialization.

Results of the CFD model baseline case with the nozzle disengaged were compared with a highly-idealized analytical mass flow rate calculation based on isentropic convergence of the flow from (assumed) stagnation conditions in the target to the inner pipe diameter. The mass flow rate for that idealized calculation was found to be 0.0646 g/s. The mass flow rate for the baseline Fluent calculation, when converted from the two-dimensional computational geometry to a pipe geometry of the calculation is 0.0471 g/s. The difference is 27 percent. However, the Fluent calculation includes geometry, turbulence, and boundary layer effects not accounted for in the idealized isentropic calculation. Each of these effects in the Fluent calculation act to reduce the computed flow rate from the idealized prediction. The mass flow rate predicted by analytical calculations is further reduced if the pipe length is taken into account via Fanno flow. Overall the Fluent results are consistent with simplified analytical model results.

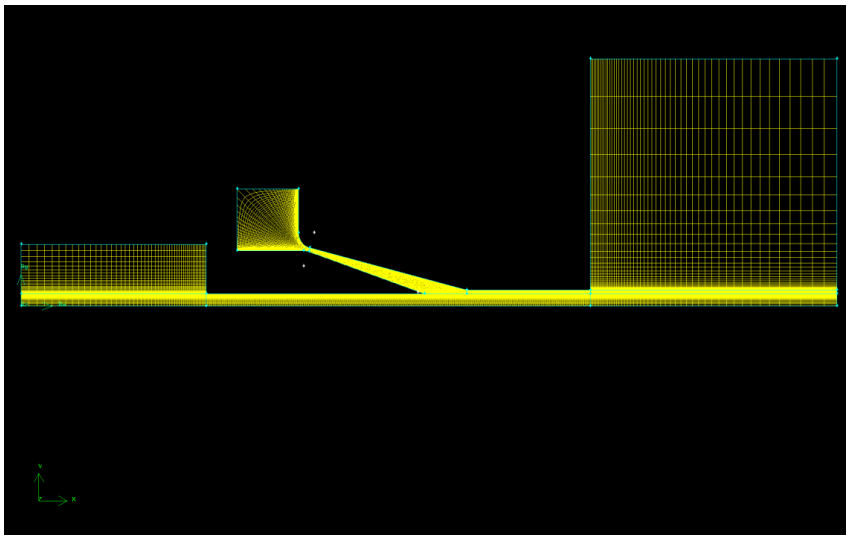

Figure 4: Nozzle-0 axisymmetric mesh.

This axisymmetric CFD model was run with a 10-Torr target and 50 mTorr vacuum port pressure. The performance curve generated by varying the inlet pressure and recording the change in mass flow rate is shown in Figure 5. In the axisymmetric case, no minimum was found over a pressure range from 10 Torr to 1950 Torr. The leakage mass flow rate increases approximately linearly with increasing nozzle inlet pressure over the whole range of pressures.

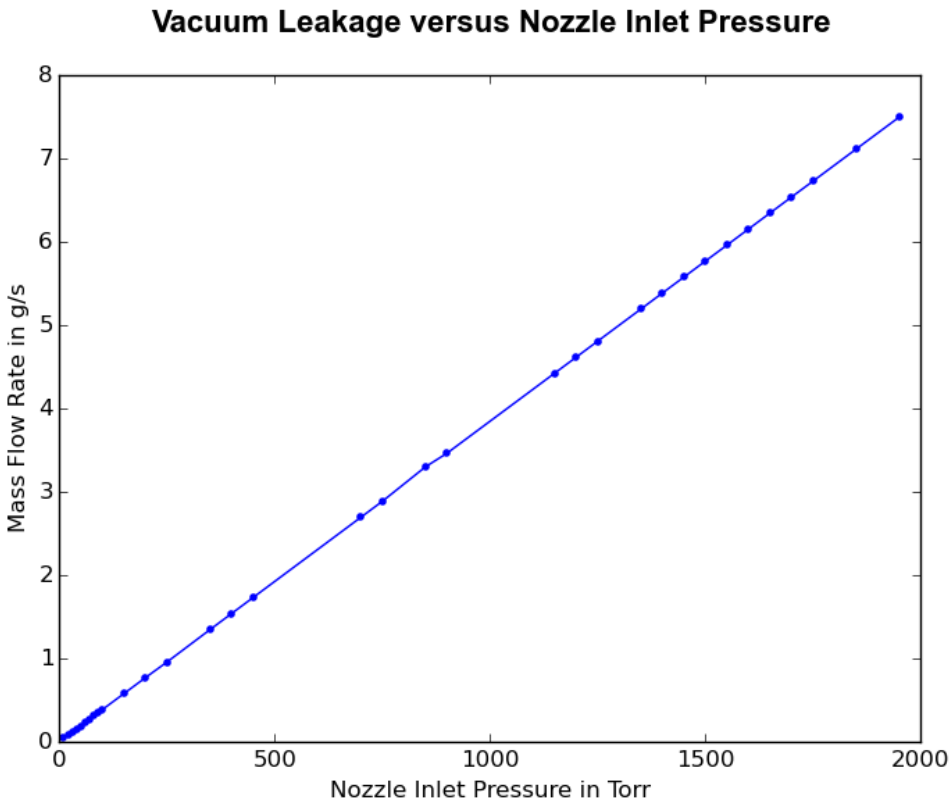

Figure 5: Nozzle-0 axisymmetric model results. No minimum was found.

In the range of nozzle inlet pressures considered, the predicted operation of the nozzle found no reduction in leakage flow. It was concluded that the nozzle-0 design was unsuited for reducing flow leakage into the vacuum port.

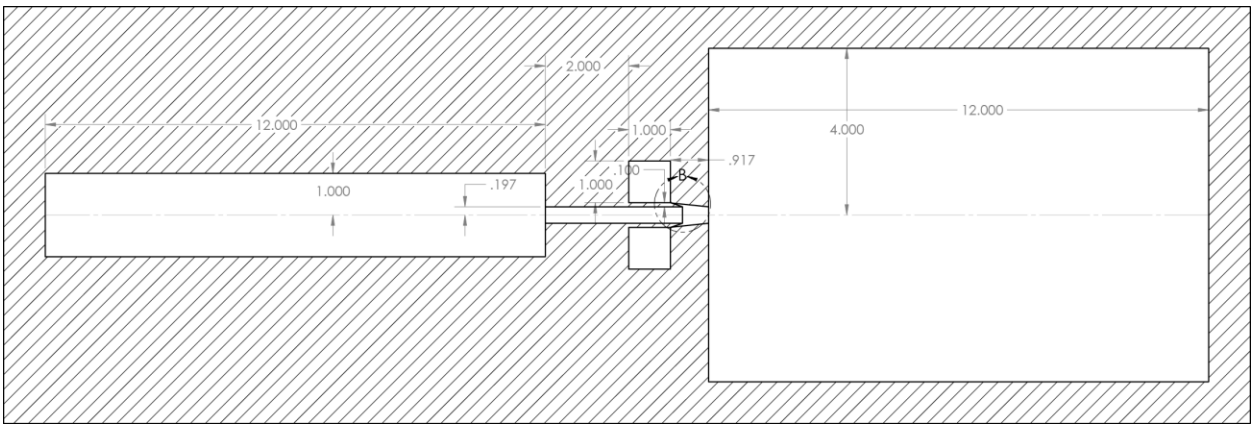

Figure 6: Nozzle-7 target assembly model specifications and dimensions.

A second design was then considered, denoted nozzle-7 and shown in Figure 6. The nozzle-7 design was evaluated for leakage reduction performance using the procedure of meshing with Ansys Gambit, preparing a CFD model with Fluent, and varying the inlet pressure at the top of the plenum and recording the change in the vacuum port leakage.

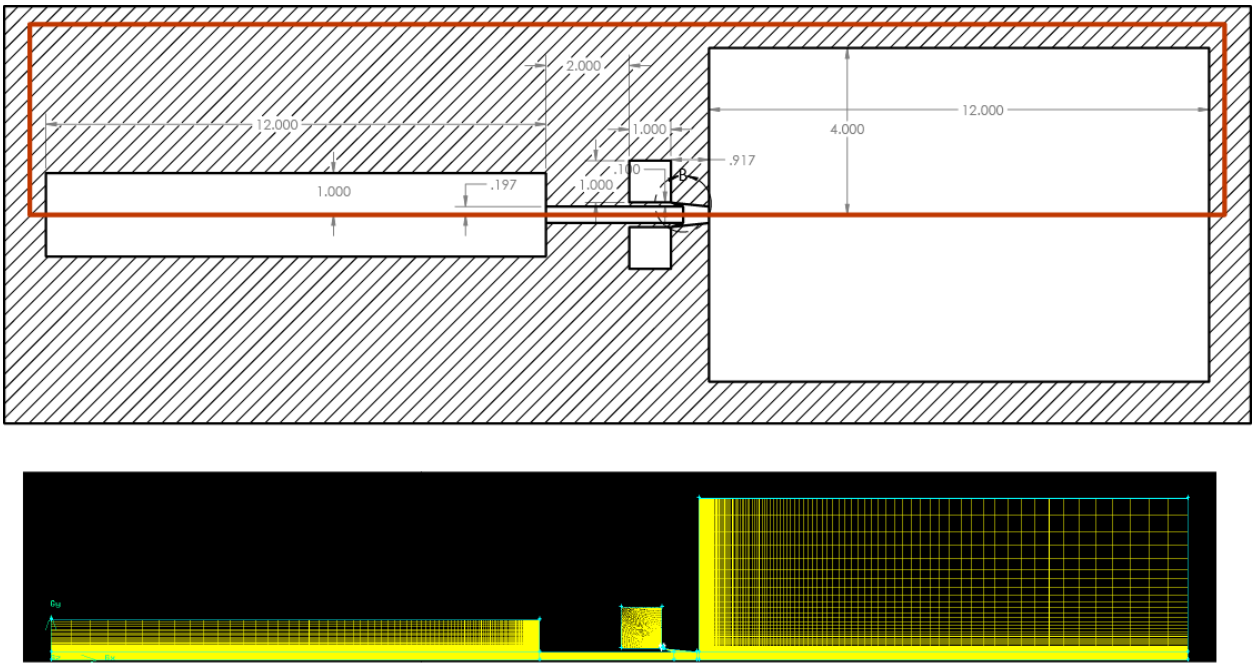

Figure 7: Nozzle-7 assembly Gambit mesh.

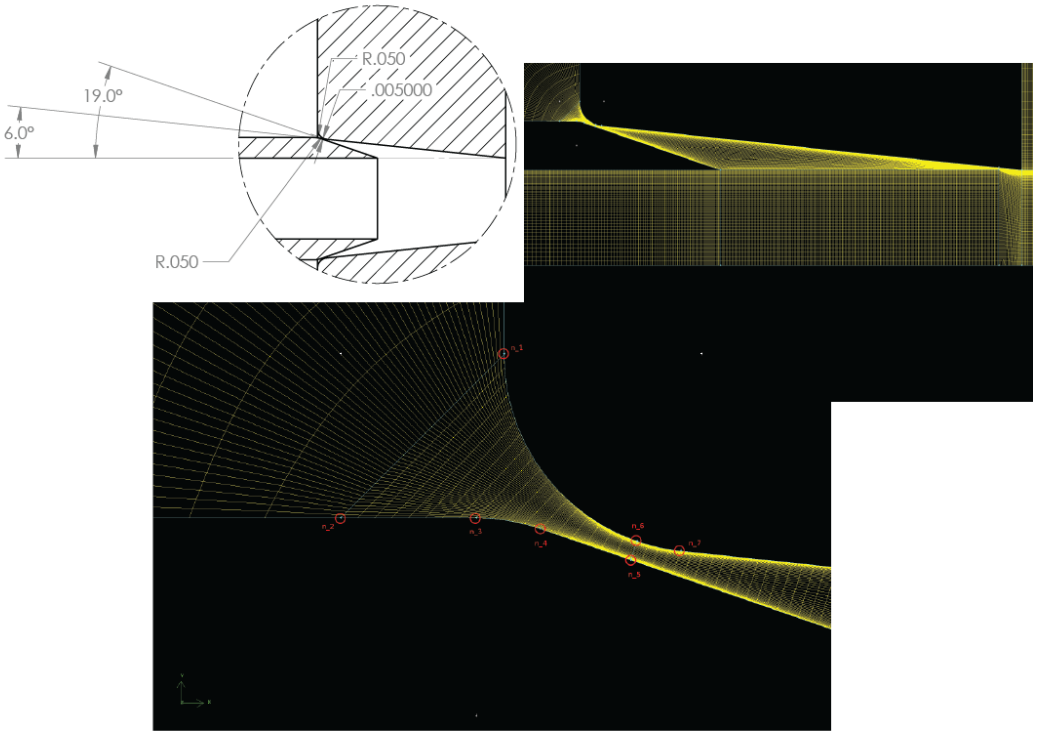

Figure 8: Nozzle-7 specifications and meshing detail.

The Gambit mesh derived from the geometric specifications is shown in Figure 7 and Figure 8.

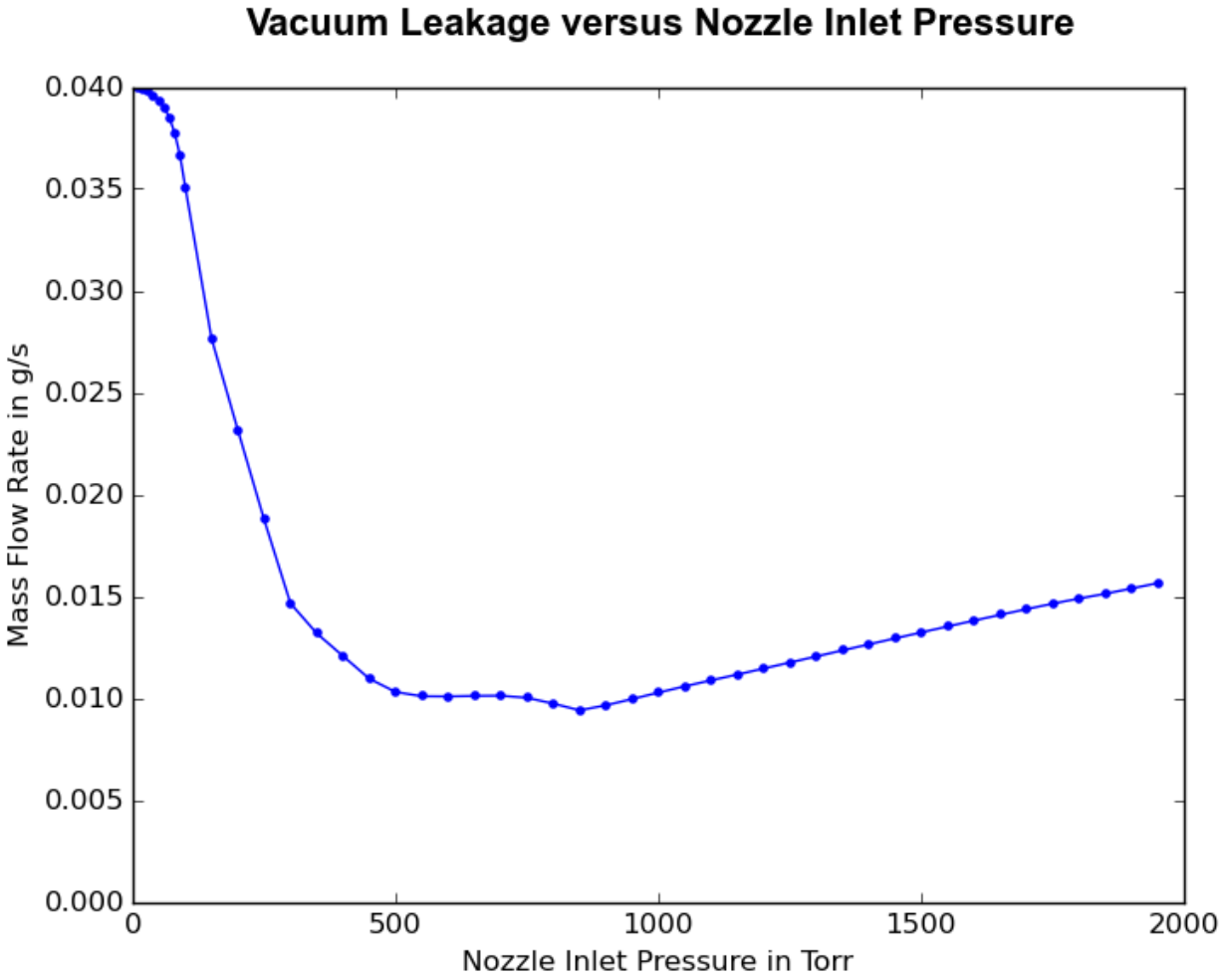

Figure 9: Nozzle-7 performance curve. The axisymmetric nozzle is effective in reducing leakage.

The results of the CFD parameter study for nozzle-7 are shown in Figure 9. The nozzle-7---design calculations indicate that the nozzle reduces the leakage of hydrogen into the vacuum port. Further, the design offers good reduction of leakage over a range of pressures varying from 500 Torr to 1000 Torr. The minimum leakage for nozzle-7 occurs at 850 Torr. Based on these positive results, the effect of varying the attachment point of the nozzle to the central pipe was studied.

Varying the geometry enables the optimal configuration to be found for ideal fluid performance. Nozzle-7 is an axially symmetric design which allows analysis to be performed on a portion of the design to evaluate complete fluid properties. The geometric portion of nozzle-7 that was manipulated was established as a quarter section of the full circular nozzle (Figure 10). Geometry was mainly changed around the nozzle inlet, outlet, and plenum (Figure 11). Other areas remained a constant so that the different models could be evaluated with the same characteristics. The geometry was isolated for the interior walls of the nozzle and dimensions were changed from this sketch (Figure 12). Once the geometry in the CAD model had been changed to desired dimensions, an extruded body was created to

represent the geometry (Figure 13). This model was converted to a step file which is supported by the mesh generation software Gambit. This method of geometry manipulation within the 3D CAD nozzle eased the creation of model iterations, and reduced the time in creating designs for fluid analysis. It was beneficial in designing specific model configurations and accurately evaluating the mechanical design of each nozzle. Further configurations could be analyzed using this design method to achieve an efficient and optimal nozzle.

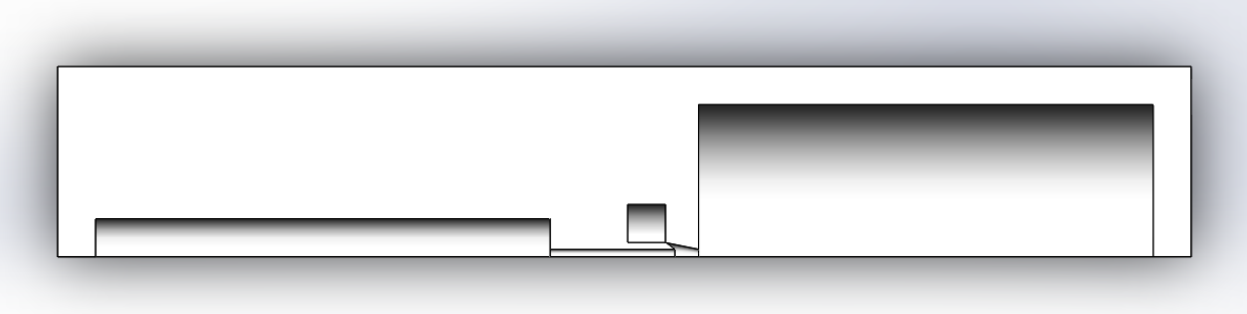

Figure 10: This section view shows a quarter of the initial geometry of Nozzle 7 which was used for each iteration.

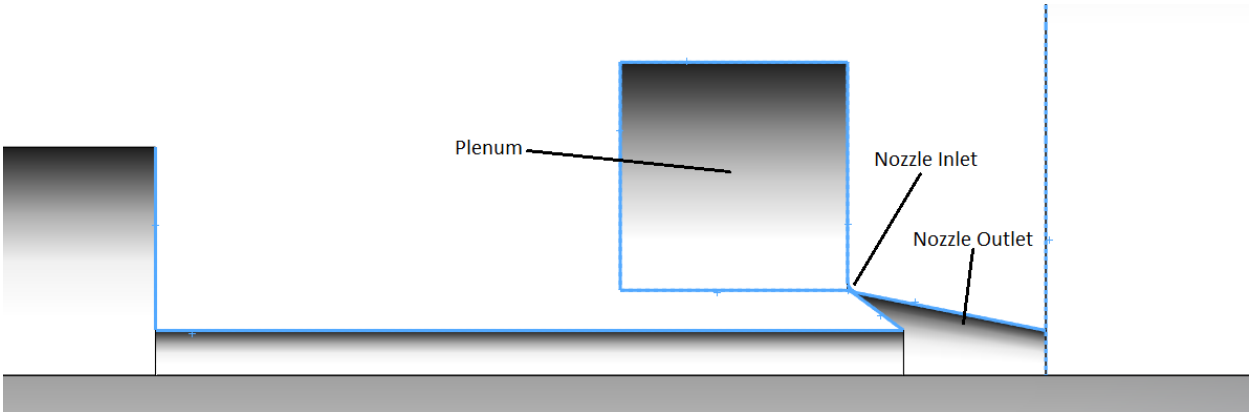

Figure 11: The highlighted portions shows where dimensions were changed in the model iterations.

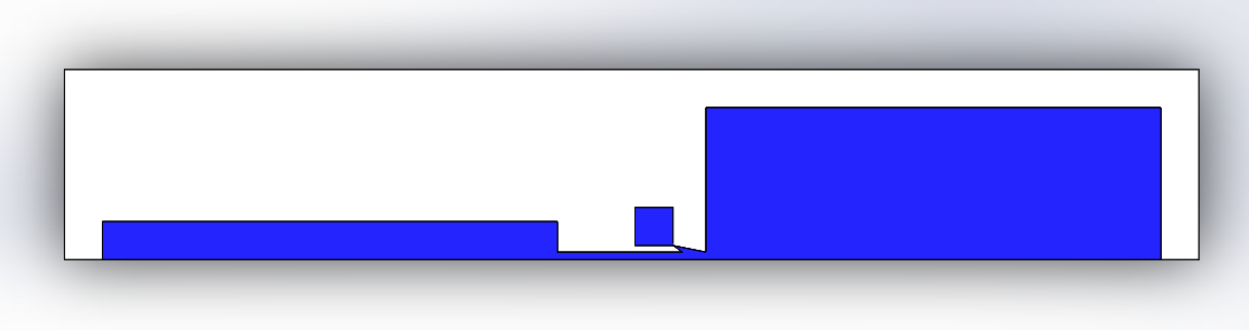

Figure 12: The highlighted portion of the design was isolated and altered in order to observe geometry effects.

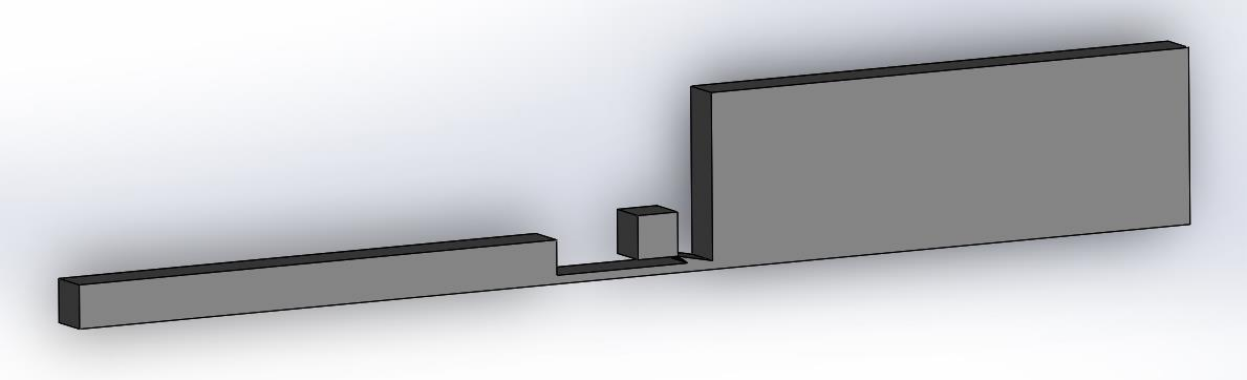

Figure 13: The extruded body shown represents the isolated geometry of the nozzle, and was converted to a .STEP file for analysis in GAMBIT.

The iterations of the nozzle to date are listed below with dimensions and brief descriptions of the variation from the original Nozzle-7 (Table 1). Columns two through five correspond to dimensions shown in Figure 14.

Model Version	*Dimension A (Inches)*	*Dimension B (Inches)*	*Dimension C (Inches)*	*Dimension D (Inches)*	*Model Geometry Description*
Original	0.100	1.100	2.000	0.916839	Original
R1	0.100	1.100	2.300	0.616839	Nozzle shifted right 0.3”
R2	0.200	1.200	2.000	0.916839	Nozzle shifted up 0.1”
R4	0.100	1.100	0.100	2.816839	Plenum 0.1” from left wall of vacuum chamber
R5	0.100	1.100	0.400	2.516839	Plenum 0.4” from left wall of vacuum chamber
R7	0.100	1.100	1.200	1.716839	Plenum 1.2” from left wall of vacuum chamber
R8	0.100	1.100	1.600	1.316839	Plenum 1.6” from left wall of vacuum chamber

Table 1: Geometry Descriptions with dimensional and model descriptions.

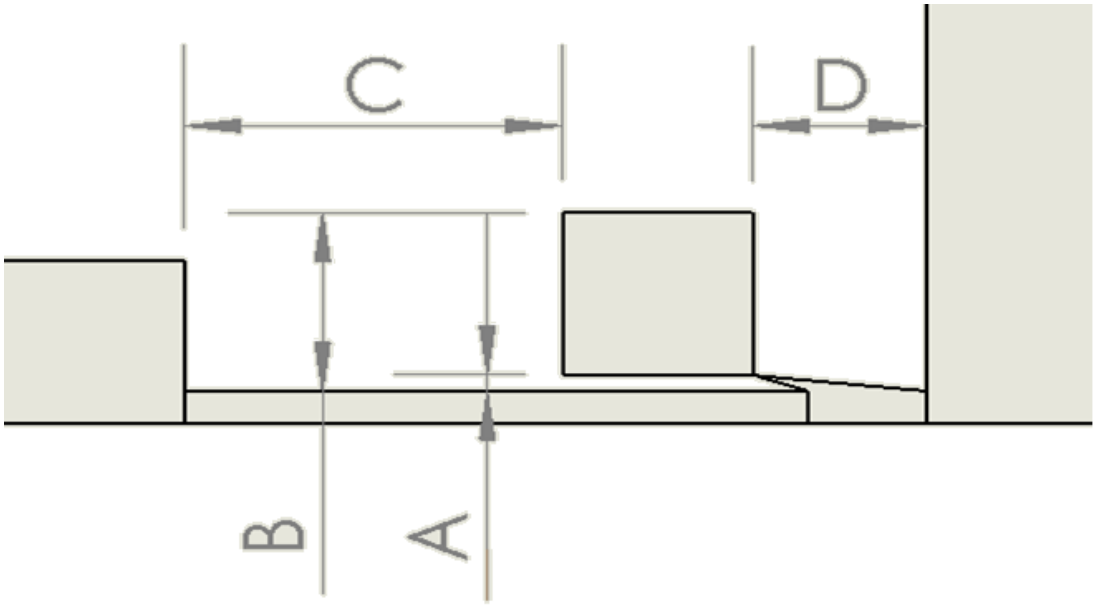

Figure 14: The dimensions listed in Table 1 are referenced from the areas indicated above.

For each version shown in the table, a series of steady-state solutions were computed with Fluent for varying nozzle reservoir pressures and target pressures. Nozzle reservoir inlet pressure was varied and the resulting behavior of steady-state mass flow rate through the vacuum chamber boundary was recorded. For each computation, explicit under-relaxation factors were set and the particular values chosen were important for simulation convergence. Convergence was determined by monitoring computed residuals for continuity, x-velocity, y-velocity, energy, k, and omega at each iteration. Solutions were only admitted as converged when residuals were less than 10^{-6}. In addition, the overall mass conservation was monitored and solutions were required to balance mass flow between the nozzle pressure inlet condition, the vacuum (LHS) pressure outlet condition, and the target (RHS) pressure outlet condition to less than 0.01 %.

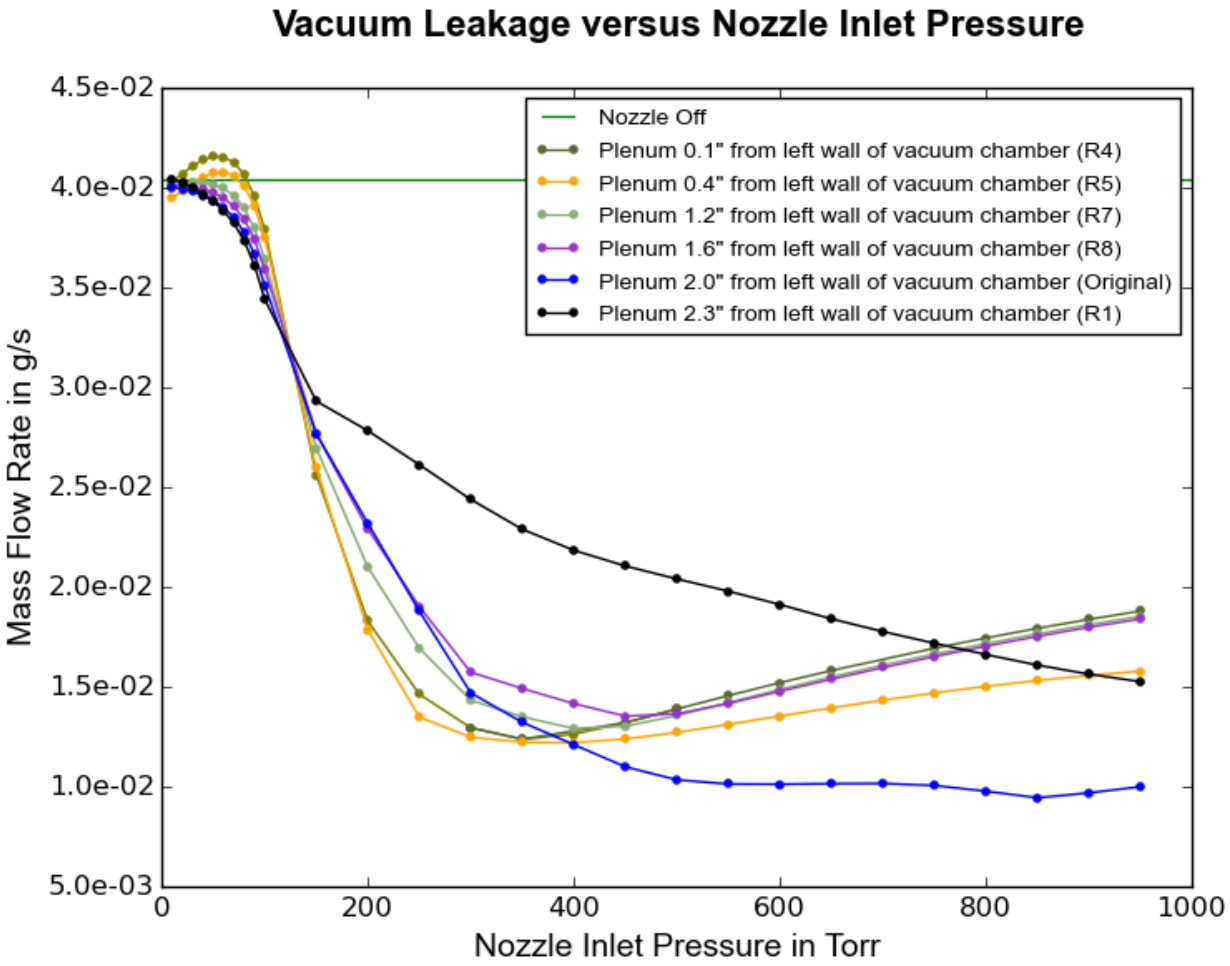

Figure 15: Leakage versus nozzle inlet pressure for nozzle attached at different points along the central pipe.

The performance of each geometry described in Table 1 is shown in Figure 15. Each point on the plot indicates a separate Fluent CFD calculation run until convergence to steady state. In general, the original attachment point was optimal for reducing leakage with an operating plenum inlet pressure of above 400 Torr. For operating pressures of 200—400 Torr, placing the assembly such that the left plenum wall was 0.4 inches from the vacuum port (case R5) was optimal, but it did not reduce the leakage as much as the original nozzle operating in the 400—1000 Torr range.

Material Properties

All previous nozzle modeling was performed considering hydrogen and constant material properties. However, the proposed nozzle would operate using deuterium or tritium during production. SHINE requested to know the effect of changing material properties and incorporating temperature dependence on the nozzle-design process. Temperature variations in the nozzle and target assemblies have been weak in the design work performed in previous studies. However, future work will involve heating due to beam dissipation where temperature changes may be significant. Temperature-dependent material properties models for deuterium and hydrogen were developed. A model of dynamic viscosity using the zero density

approach of Assael, et. al.[4] was developed. A dynamic viscosity User Defined Function (UDF) was written in C and incorporated into Fluent. The model is shown in Figure 16.

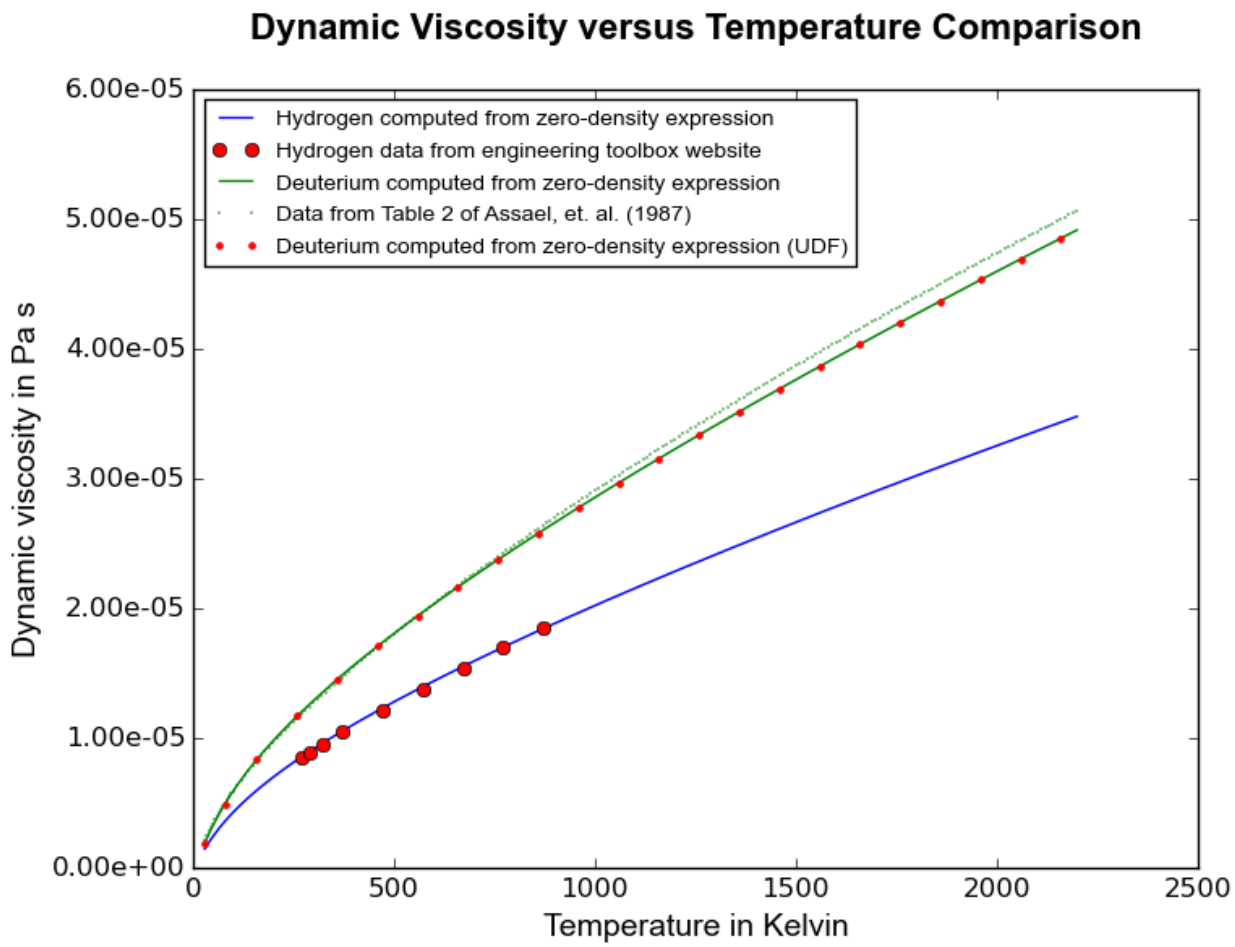

Figure 16: Comparison of zero-density expressions and UDF for dynamic viscosities of hydrogen and deuterium.

Data for thermal conductivity and specific heat were provided by PNL based on tabular EES data. These tabulated data were incorporated into UDFs and linear interpolation was implemented in each UDF to provide continuous temperature dependent properties. The thermal conductivity data and specific heat data are shown in Figure 17 and Figure 18, respectively.

[4] The Viscosity of Normal Deuterium in the Limit of Zero Density. Assael, et al. J. Phys. Chem. Ref. Data, 16-2 (1987).

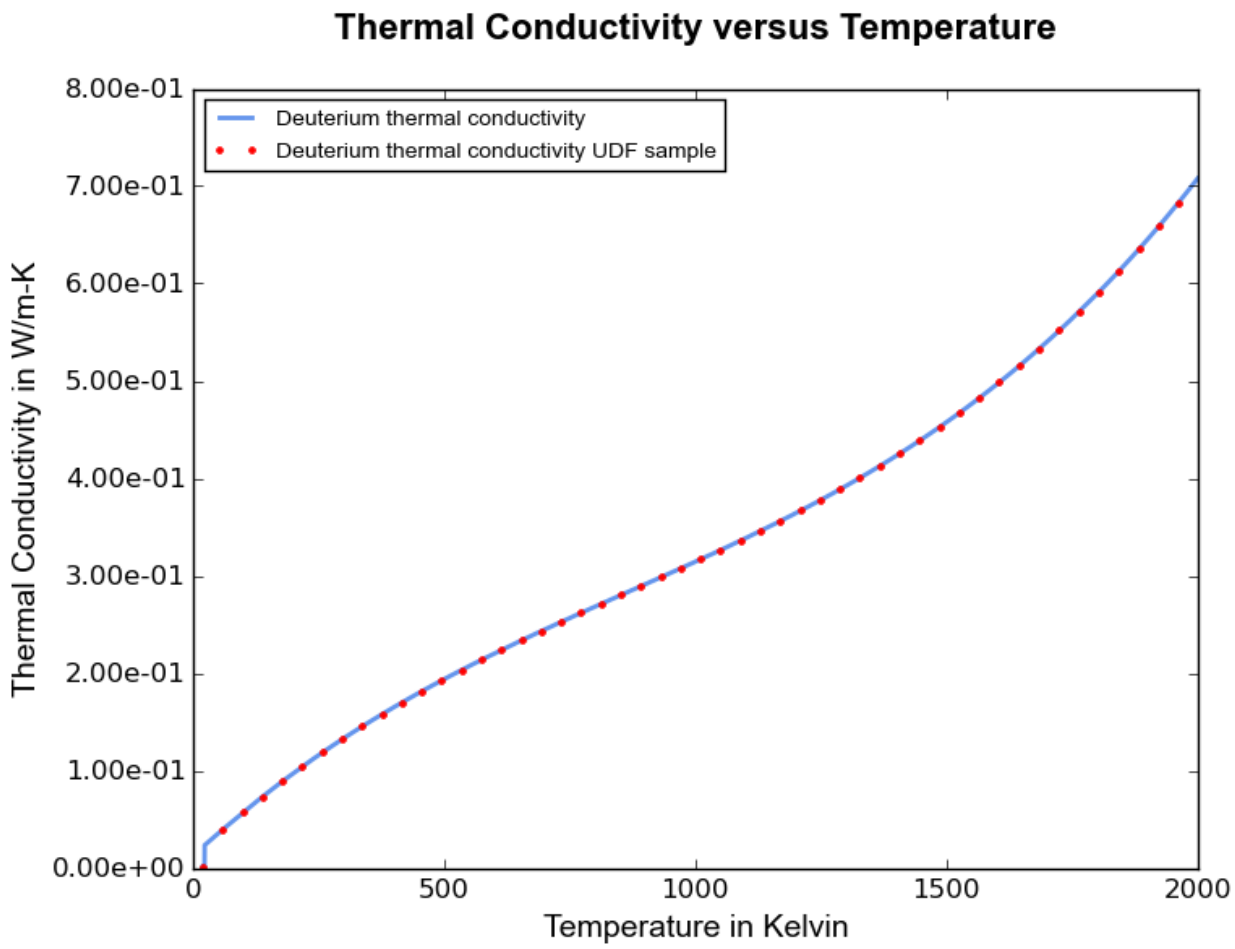

Figure 17: Thermal conductivity generated from UDF in Fluent based on tabular data.

The specific heat data shown in Figure 18 shows some oscillatory behavior for low temperatures. The provenance of this data should be investigated further, however none of the calculations reported here had temperatures in the range of the oscillations.

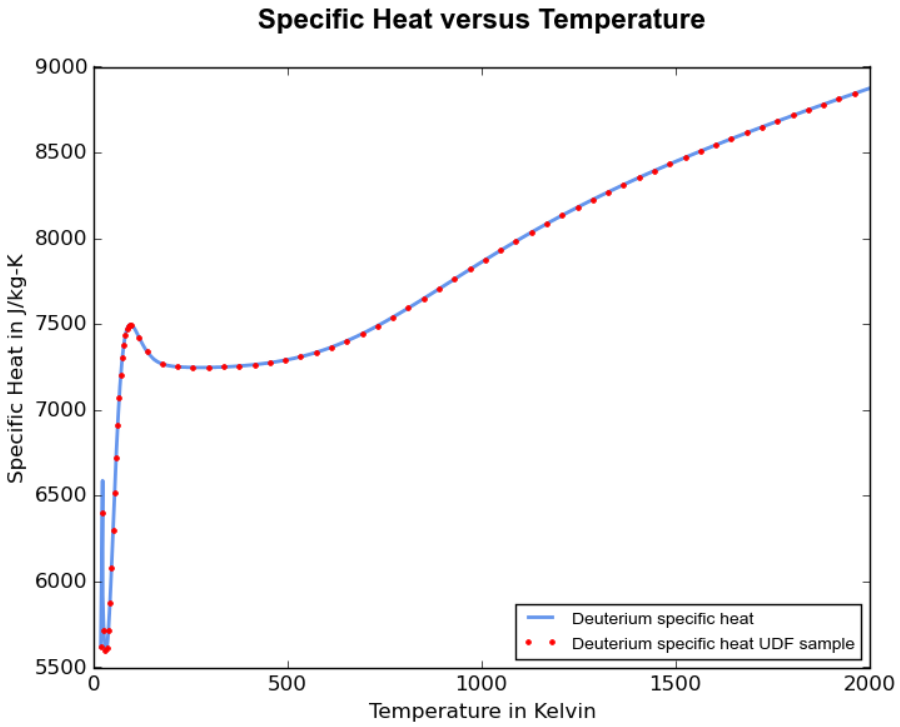

Figure 18: Specific heat for deuterium implemented as a UDF in Fluent based on tabular data.

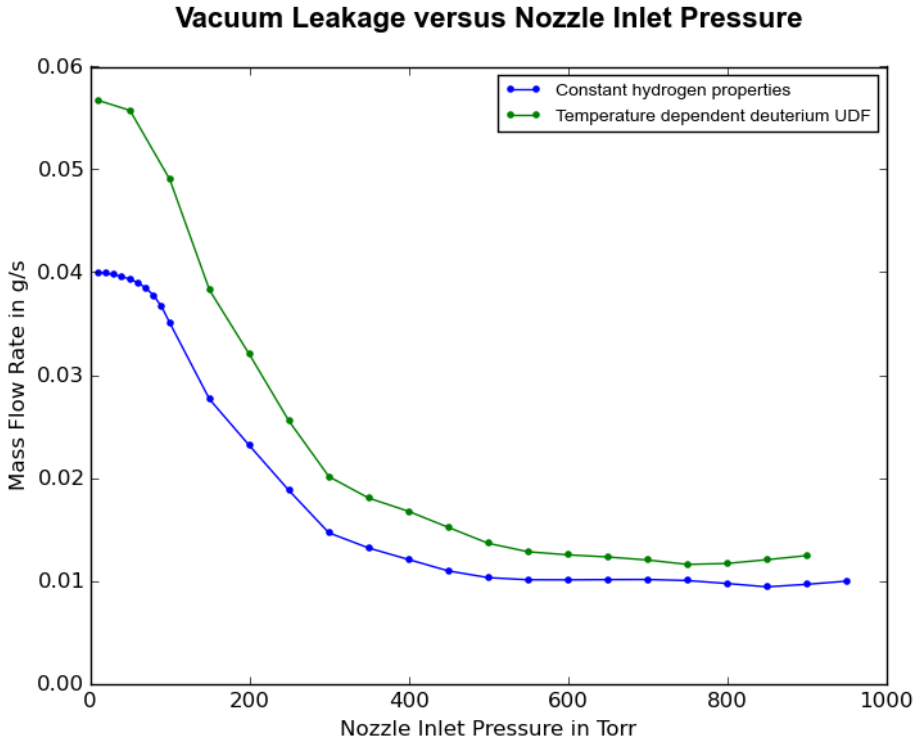

Figure 19: Comparison of constant hydrogen properties to temperature-dependent deuterium properties.

A comparison of performance for hydrogen and deuterium was performed. The results are shown in Figure 19. The nozzle performance is qualitatively similar in both cases. The minimum flow rate for the hydrogen case occurred at 850 Torr. The minimum deuterium flow rate was computed at 750 Torr. In both cases the curves are relatively flat in the range of 550—900 Torr. The quantitative leakage rates for deuterium are higher, due to the higher density of deuterium. The temperature variation in these calculations is not significant, however in system with a beam engaged this is not likely to be the case and more differences due to temperature variations would be expected. After performing parameter scans with hydrogen and deuterium, SHINE desired to use a common set of material properties for hydrogen. The constant properties provided by SHINE for use in the comparison calculations are shown in the table below.

Property	Value
Viscositv	9.1e-6 Pa s
Specific Heat (Cp)	14310.5 J/(kg K)
Thermal Conductivity	0.187 W/(m K)

These properties were used for the calculations shown in Figure 15.

Conclusions

Previous results with a two-dimensional Cartesian nozzle showed that the nozzle reduced flow into the vacuum port from a baseline no-nozzle configuration. However, when an axisymmetric nozzle with the same two-dimensional cross section was analyzed, increasing the plenum inlet pressure only increased the leakage mass flow rate into the vacuum port. Axisymmetric designs are preferable for integrating into the existing bellows, therefore a new axisymmetric design was considered. The new design, nozzle-7, reduced the nozzle throat size, moved the nozzle assembly closer to the target, and reduced the nozzle angle. The new design reduced the leakage into the vacuum port for sufficiently high plenum inlet pressures. As the inlet pressure was increased further, leakage increased with pressure.

To study the geometric design space of the nozzle, LANL varied the location of the attachment point along the central pipe. For each location, a performance curve was generated. In general, the original attachment point was optimal for reducing leakage in an operating range of 400 Torr and above. For operating pressures of 200—400 Torr, placing the assembly such that the left plenum wall was 0.4 inches from the vacuum port (case R5) was optimal, but it did not reduce the leakage as much as the original nozzle operating in the 400—1000 Torr range.

Fluent User-Defined Functions (UDFs) were constructed for using material properties of deuterium instead of hydrogen. The effect of using deuterium material properties was qualitatively similar and differences were quantitatively small. Therefore the work analysis was performed with hydrogen.

An operational nozzle reservoir inlet pressure was discovered which minimizes leakage while maximizing the pressure drop across the bellows for a10-Torr target.

Future Work

LANL recommends further study of the nozzle and its exit region within the PNL beamline. The effect of heat generated due to power dissipation of the beam needs to be incorporated into the CFD model. The addition of heat may have a significant effect on the fluid behavior and, thus the nozzle performance for leakage mitigation.

Mechanisms of vacuum chamber mass flow rate control have been identified, but these mechanisms need to be explored so that they may be exploited optimally in a final nozzle design for production. With a quantitative knowledge of the mechanisms involved, the features of an optimal nozzle will be more apparent. LANL suggests that the proposed nozzle be redesigned to incorporate the knowledge and experience gained in the present study.

LANL also recommends the flow in the nozzle exit region be further studied at additional target pressures. An operational nozzle reservoir inlet pressure was discovered which minimizes leakage while maximizing the pressure drop across the bellows for a10-Torr target. LANL suggests performing experiments in conjunction with simulation and incorporating additional real-world features in to the CFD simulations. The geometry and boundary conditions in the vacuum port and target chambers should be investigated and evaluated to ascertain that the flow being predicted is a good model of the actual flow. For example, the pressure boundary conditions are not far field and may influence the simulated flow. Also, when Fluent encounters a shock in the computed flow, it can no longer enforce the boundary condition upstream of the shock, which raises questions about the pressure in the vacuum port. A continuum representation of the flow regime in the system to the left of the nozzle is likely a coarse approximation of the flow regime. The flow in this area does not satisfy the assumptions of the continuum regime that the CFD is based upon. There is likely a transition between the continuum representation appropriate at the nozzle exit, and the flow in the vacuum port. The basic results reported here are adequate representations of the flow phenomenology for evaluating nozzle performance, however for investigating the larger system at higher fidelity, some capability that allows simultaneous simulation in both flow regimes needs to be developed and incorporated into the analysis.